Supporting Information

Incorporation of Clathrochelate-Based Metalloligands in Metal-Organic Frameworks by Solvent-Assisted Ligand Exchange

Ophélie M. Planes,[#] Pascal A. Schouwink,[#] José L. Bila,[#] Farzaneh Fadaei-Tirani,[#] Rosario Scopelliti[#] and Kay Severin*[,#]

[#] Institute of Chemical Sciences and Engineering, Ecole Polytechnique Fédérale de Lausanne (EPFL), CH-1015 Lausanne and CH-1951 Sion, Switzerland

Table of contents

General

All commercially available chemicals and solvents were used without further purification. Reactions were carried out under an atmosphere of N_2 using standard Schlenk techniques. Routine ^{1}H NMR and ^{13}C NMR spectra were obtained on a Bruker Avance III Spectrometer equipped with a 5 mm BBFO-Plus$_z$ probe and at 298 K. ^{1}H and ^{13}C shifts are reported in parts per million (ppm δ) referenced to the internal solvent. Electrospray-ionisation MS data were acquired on a Q-Tof Ultima mass spectrometer. Thermogravimetric analyses (TGA) were performed on a TGA 4000 from Perkin Elmer. Samples were placed in crucibles and heated from 30 °C to 700 °C at 10 °C/minute under N_2. Powder X-ray diffraction (PXRD) patterns were recorded at room temperature with a Bruker D8 Discover diffractometer equipped with a LynxEye XE detector using non-monochromated Cu-radiation. Due to the sample nature, MOFs **3a, 3b, 3c**, **3d**, **5** and **7** were measured in transmission (Debye-Scherrer, 1.0 mm borosilicate capillary, spun at 30 rpm). Data are shown as measured. The samples were loaded without grinding (lack of mechanical stability of the crystal structure) into borosilicate glass capillaries of 1 mm diameter, together with the mother liquor, to prevent collapse during measurement. Capillaries were spun during measurement.

Synthetic procedures

Ligands **2a** and **2c** were synthesized following published procedures.[1, 2]

Ligand 2b:

$FeCl_2$ (308 mg, 2.43 mmol), diethylglyoxime (1.05 g, 7.30 mmol) and pyridine-4-boronic acid (598 mg, 4.87 mmol) were dissolved in MeOH (135 mL). The mixture was heated to reflux during 3 h under N_2. The solution was cooled to RT, and the solvent was removed under reduced pressure. Subsequently, the resulting solid was dissolved in DCM (40 mL). The organic phase was washed with a saturated solution of $NaHCO_3$ (100 mL), dried ($MgSO_4$), and filtered. Removal of the solvent under vacuum gave **2b** in the form of a red powder (0.74 g, 46%).

^{1}H NMR (400 MHz, CD_2Cl_2) δ : 8.54 (s, 4H, C_{arom}), 7.59 (s, 4H, C_{arom}), 2.83 (q, J = 7.5 Hz, 12H, CH_2), 1.17 (t, J = 7.5 Hz, 18H, CH_3). **^{13}C{^{1}H} NMR** (101 MHz, CD_2Cl_2) δ : 158.91 (C_{arom}), 149.09 (C_{arom}), 127.39 (C=N), 21.43 (CH_3), 11.77 (CH_2) (C-B not detected). **HRMS (ESI TOF)** $[M+H]^+$ calcd for $[C_{28}H_{39}B_2FeN_8O_6]^+$ 661.2537, found 661.2552.

Ligand 2d:

$FeCl_2$ (149 mg, 1.18 mmol), R-pulegone dioxime (551 mg, 3.53 mmol)[3] and pyridine-4-boronic acid (289 mg, 2.35 mmol) were dissolved in MeOH (140 mL). The mixture was heated to reflux during 3 h under N_2. The solution was cooled to RT, and the solvent was removed under reduced pressure. The resulting solid was dissolved in DCM (15 mL) and sonicated for 5 min. A filtration through silica gave an orange solution, which was evaporated under reduced pressure. Subsequently, the resulting red-orange solid was dissolved in DCM (40 mL). The organic phase was washed with a saturated solution of $NaHCO_3$ (100 mL), dried ($MgSO_4$), and filtered. Removal of the solvent and drying under vacuum for 14 h gave **2d** in the form of a red powder. Despite the drying step, the final product contained some water, as evidenced by NMR spectroscopy. The water (2 was taken into account for calculating the yield (793 mg, 92%). It is expected that **2d** is present as a mixture of *mer*- and *fac*- isomers,[3] but it was not possible to distinguish them by NMR.

^{1}H NMR (400 MHz, CD_2Cl_2) δ : 8.52 (s, 4H, C_{arom}), 7.54 (s, 4H, C_{arom}), 3.17 (d, J = 19.9, 16.7, 5.6 Hz 6H, CH_2), 2.71 (ddd, J = 18.6, 11.6, 6.1 Hz, 3H, CH_2), 2.32 (dd, J = 18.7, 10.8 Hz, 3H, CH_2), 1.92 (s, 6H, CH_2), 1.46 – 1.43 (m, 3H, CH), 1.10 (d, J = 6.4 Hz, 9H, CH_3). **^{13}C{^{1}H} NMR** (101 MHz, CD_2Cl_2) δ : 153.15 (C_{arom}), 152.86 (C_{arom}), 149.08 (C=N), 127.33 (C=N), 34.58 (CH_3), 30.18 (CH), 29.15 (CH_2), 26.01(CH_2), 21.37 (CH_2) (C-B not detected). **HRMS (ESI TOF)** $[M+H]^+$ calcd for $[C_{31}H_{39}B_2FeN_8O_6]^+$ 697.2539, found 697.2538.

MOF **1** was synthesized as described in the literature.[4]

Solvent-Assisted Ligand Exchange:

Synthesis of the MOFs **3a, 3b, 3c,** and **3d**: Saturated DMF solutions of the clathrochelate complexes **2a**, **2b**, **2c** and **2d** were prepared by stirring a mixture of the respective complex (~ 75 – 96 mg) in DMF (4 mL) for 5 min at RT, followed by filtration. This procedure was repeated 7 times to obtain 28 mL of a saturated solution for each clathrochelate complexe. Crystals of MOF **1** (30 mg) were immersed in a saturated solution of the respective metalloligand (7 mL), and the mixture was heated to 80 °C for 3 d. The progress of SALE was monitored by ^{1}H NMR and UV-Vis spectroscopy.
Synthesis of the MOFs **5** and **7**: Saturated DMF solutions of the clathrochelate complex **2a** was prepared by stirring a mixture of the respective complex (~ 88 – 100 mg) in DMF (4 mL) for 5 min at RT, followed by filtration. This procedure was repeated 8 times to obtain 32 mL of a saturated solution of **2a**. Crystals of MOF **4** (20 mg) or MOF **6** (20 mg) were immersed in a saturated solution of the metalloligand **2a** (8 mL), and the mixture was heated to 80 °C for 3 d. The progress of SALE was monitored by ^{1}H NMR and UV-Vis spectroscopy.

NMR spectra

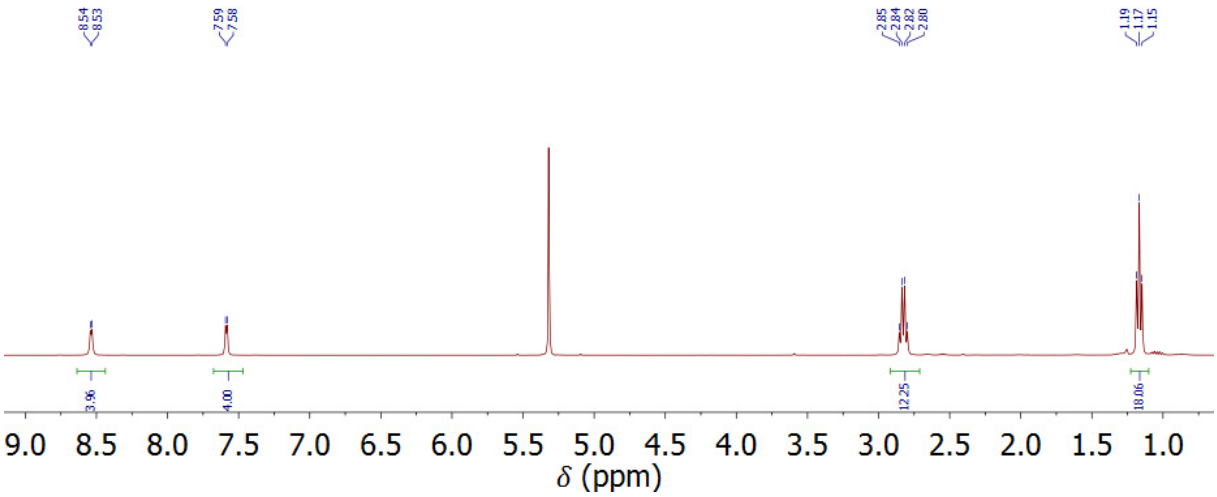

Figure S1. ^{1}H NMR of **2b** in CD_2Cl_2 (400 MHz).

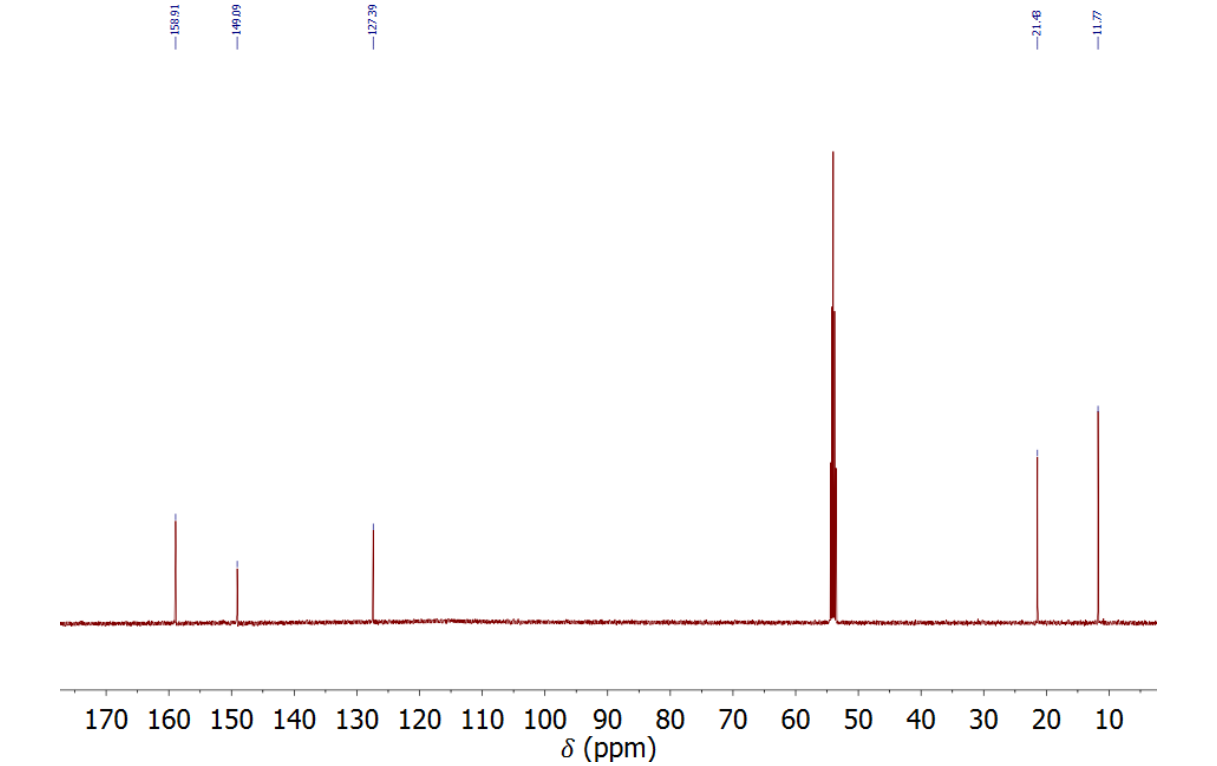

Figure S2. ^{13}C NMR of **2b** in CD_2Cl_2 (400 MHz).

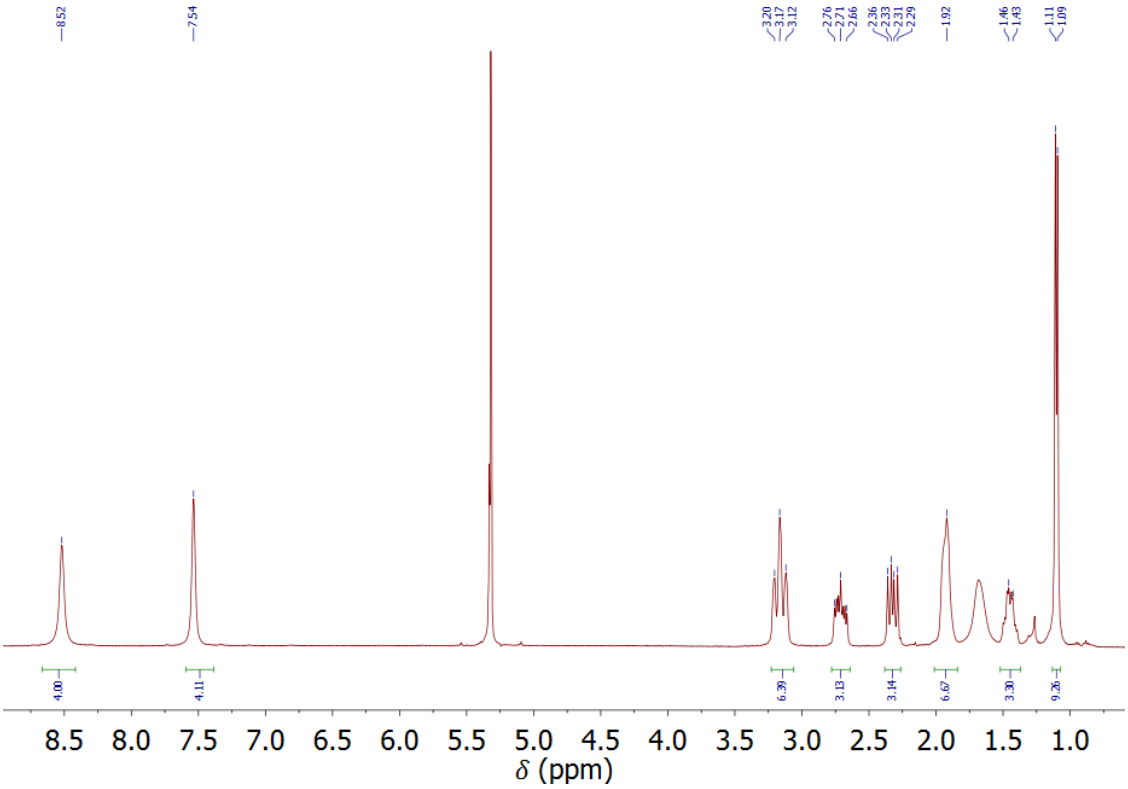

Figure S3. ^{1}H NMR of **2d** in CD_2Cl_2 (400 MHz).

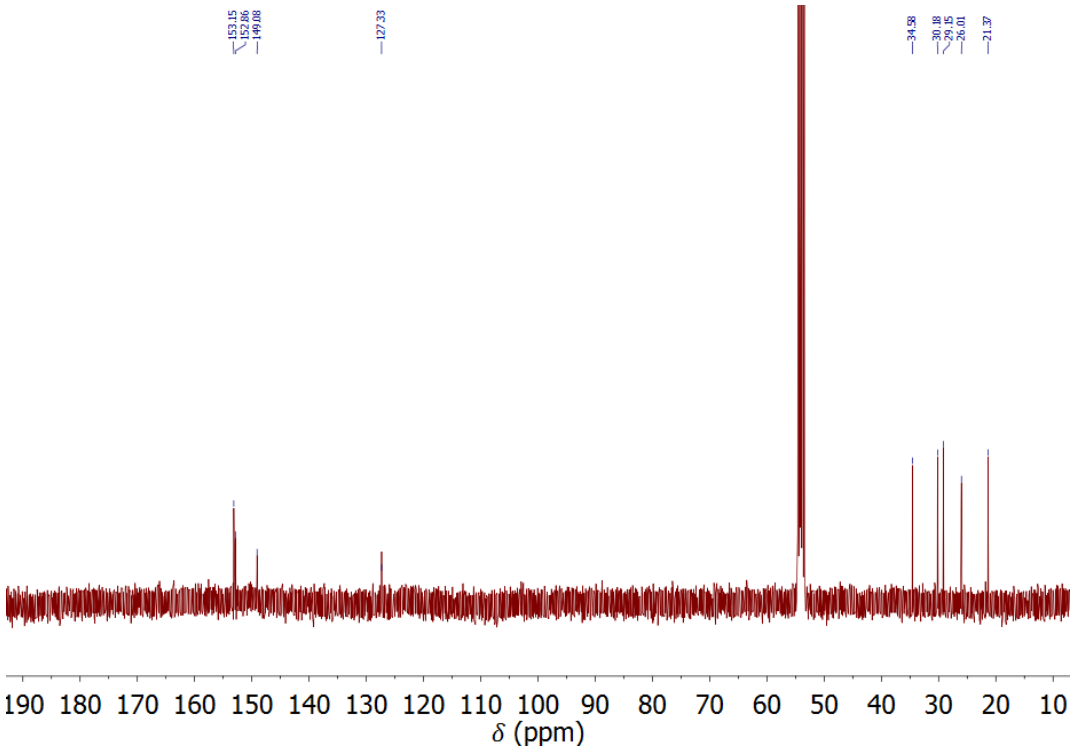

Figure S4. ^{13}C NMR of **2d** in CD_2Cl_2 (400 MHz).

Approximately 1-5 mg of MOF crystals were removed from the reaction mixture, and washed several times with DMF. The crystals were then placed in a 2 mL vial containing deuterated dimethyl sulfoxide (DMSO-d_6, 0.6 mL). 2 drops of H_2SO_4 were added, and the mixture was sonicated for 5 min to achieve complete dissolution. The sample was then transferred to an NMR tube and a ^{1}H NMR spectrum was recorded. According to the NMR spectra recorded after a reaction time of 3 days, ligand exchange is essentially quantitative (> 98%), except for **3b**, where we could detect small amounts of residual **DPNI** linker (~14%, Figure S6).

The ^{1}H NMR digestion of MOF **3d** is shown in the main text.

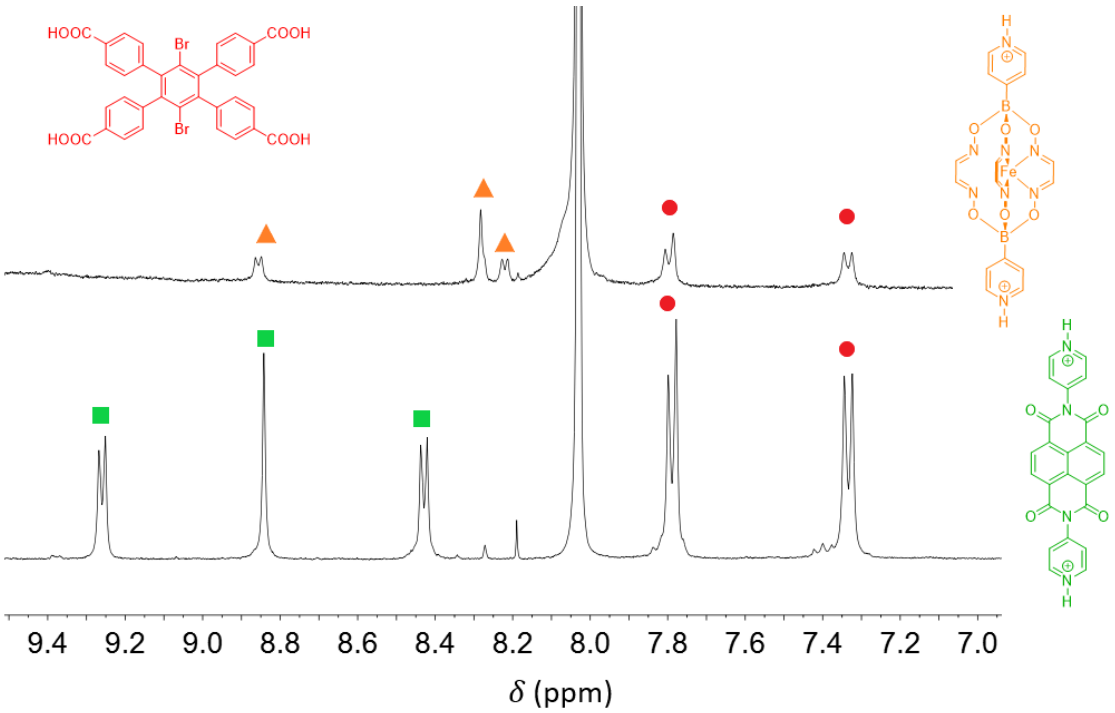

Figure S5. Progress of the conversion of **1** into **3a** as monitored by ^{1}H NMR spectroscopy (DMSO-d_6 + H_2SO_4, zoom on the aromatic region). Sample composition after 5 min (bottom), and after 3 d (top). Signals depicted in green correspond to the protonated **DPNI** linker, orange for the protonated clathrochelate **2a**, and red for the carboxylic acid ligand.

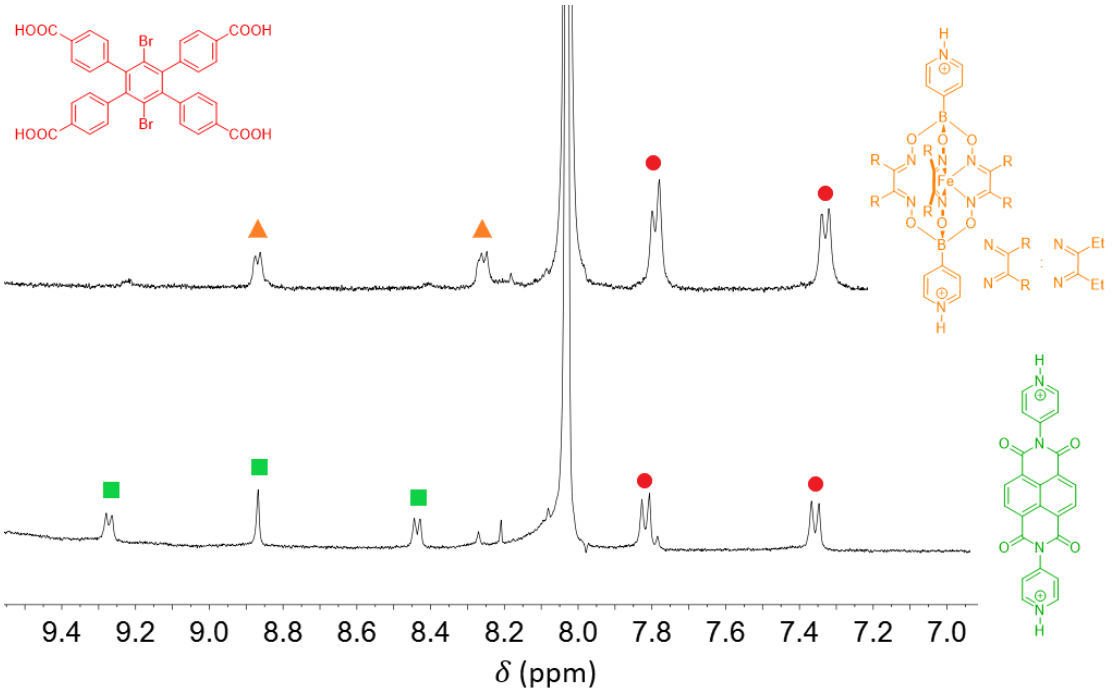

Figure S6. Progress of the conversion of **1** into **3b** as monitored by ^{1}H NMR spectroscopy (DMSO-d_6 + H_2SO_4, zoom on the aromatic region). Sample composition after 5 min (bottom), and after 3 d (top). Signals depicted in green correspond to the protonated **DPNI** linker, orange for the protonated clathrochelate **2b**, and red for the carboxylic acid ligand.

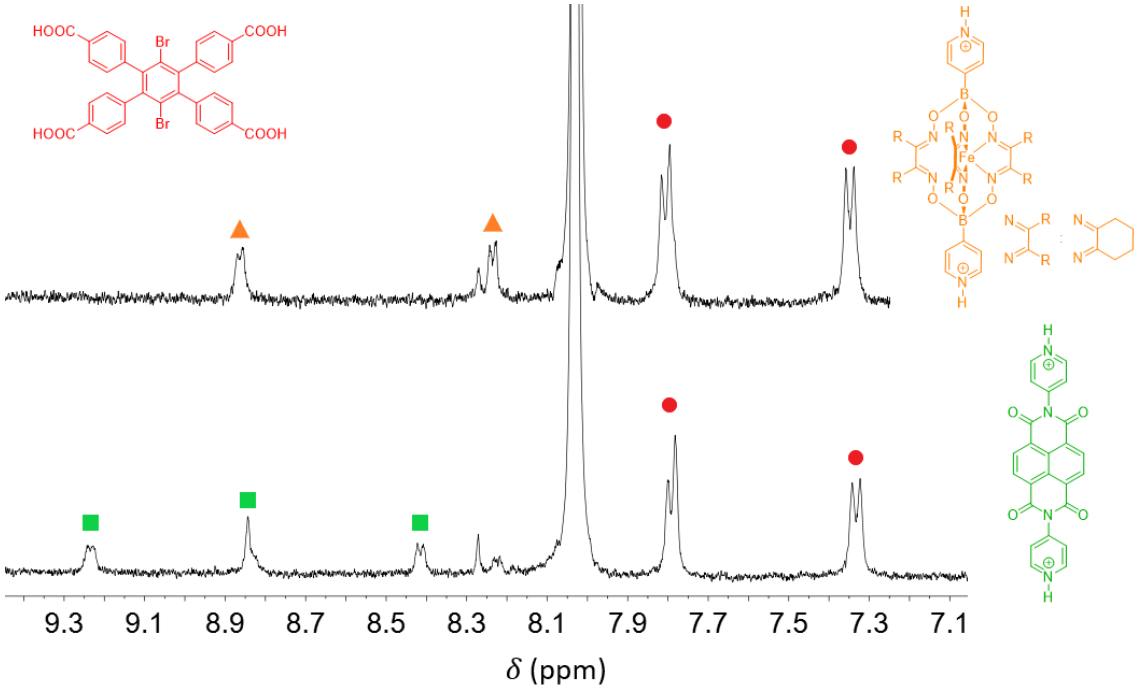

Figure S7. Progress of the conversion of **1** into **3c** as monitored by ^{1}H NMR spectroscopy (DMSO-d_6 + H_2SO_4, zoom on the aromatic region). Sample composition after 5 min (bottom), and after 3 d (top). Signals depicted in green correspond to the protonated **DPNI** linker, orange for the protonated clathrochelate **2c**, and red for the carboxylic acid ligand.

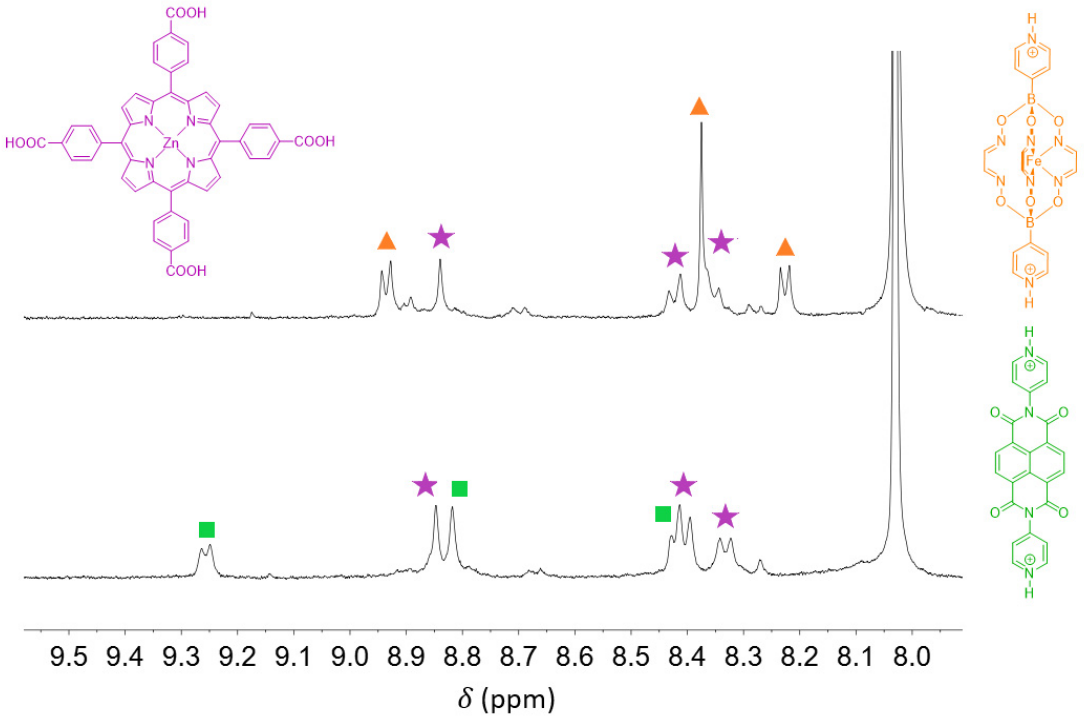

Figure S8. Progress of the conversion of **4** into **5** as monitored by ^{1}H NMR spectroscopy (DMSO-d_6 + H_2SO_4, zoom on the aromatic region). Sample composition after 5 min (bottom), and after 3 d (top). Signals depicted in green correspond to the protonated **DPNI** linker, orange for the protonated clathrochelate **2a**, and purple for the carboxylic acid ligand.

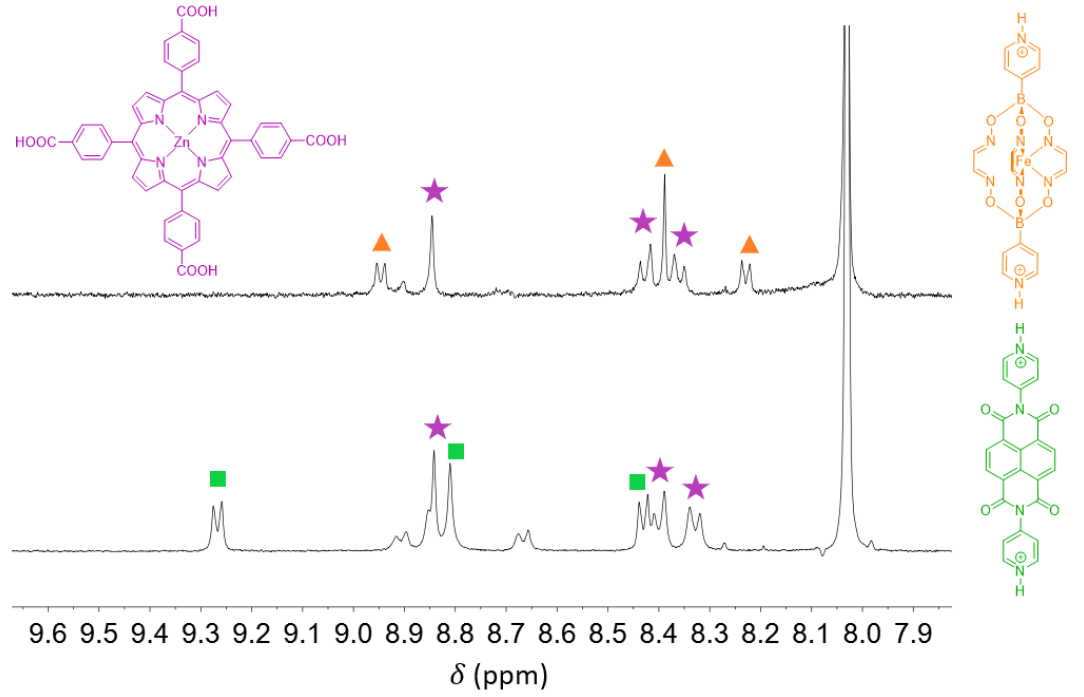

Figure S9. Progress of the conversion of **6** into **7** as monitored by ^{1}H NMR spectroscopy (DMSO-d_6 + H_2SO_4, zoom on the aromatic region). Sample composition after 5 min (bottom), and after 3 d (top). Signals depicted in green correspond to the protonated **DPNI** linker, orange for the protonated clathrochelate **2a**, and purple for the carboxylic acid ligand.

UV-Vis spectra

The SALE process was also monitored by UV-Vis spectroscopy. UV-Vis spectra of the reaction solutions were recorded after 5 min (orange) and after 3 d (green). The new bands at 360 and 380 nm indicate that **DPNI** is released in solution, whereas the absorption of the cage complex (**2a**, **2b**, **2c** or **2d**) at ~ 450 nm diminishes.

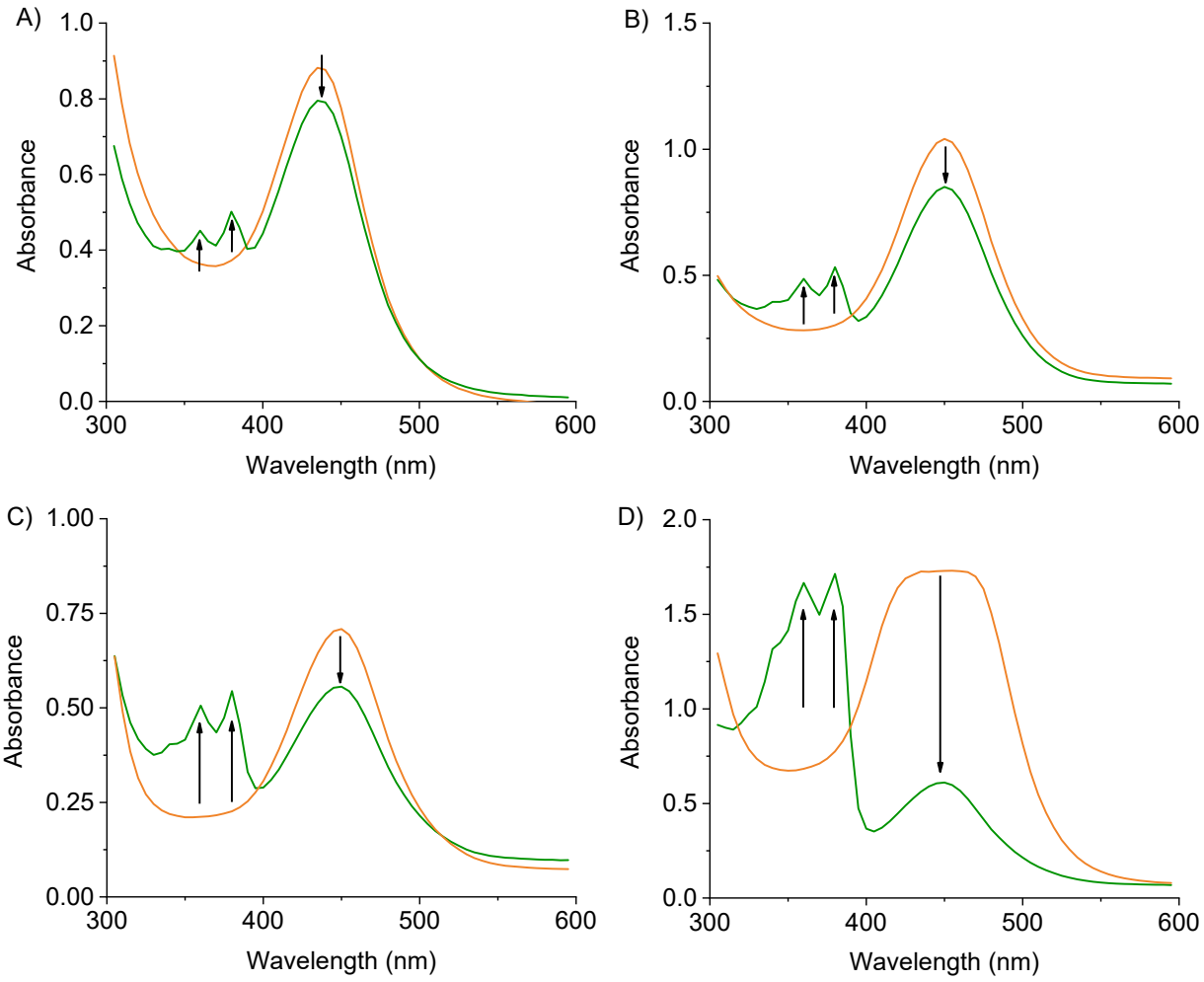

Figure S10. UV-Vis spectra of DMF solutions from SALE experiments with MOF **1** and the cage complexes 2**a** (A), **2b** (B), **2c** (C) and **2d** (D). The spectra were recorded after a reaction time of 5 min (orange), and after 3 d (green).

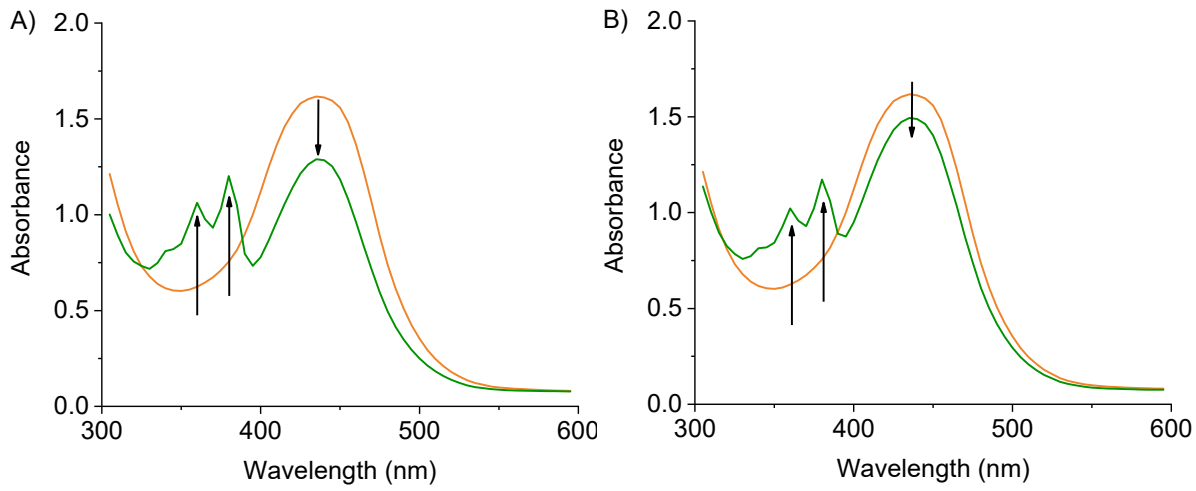

Figure S11. UV-Vis spectra of DMF solutions from SALE experiments with MOF **4** (PPF-18) and the cage complex 2**a** (A), and with MOF **6** (PPF-19) and the cage complex **2a** (B). The spectra were recorded after a reaction time of 5 min (orange), and after 3 d (green).

TGA measurements

Before the TGA measurements, samples were dried for 30 min. under vacuum. The TGA curves indicate high stabilities, with framework pyrolysis starting at ~ 330 °C for the series **3a**–**3d**, and at ~ 380 °C for **5** and **7**. The first mass loss (20–70%) corresponds to release of entrapped DMF molecules, which were not removed during the short drying period. The higher initial mass loss for **3b** indicates that solvent removal under vacuum was less efficient for this MOF. The TGA profile of MOF **1** is given in ref. 56 (main text).

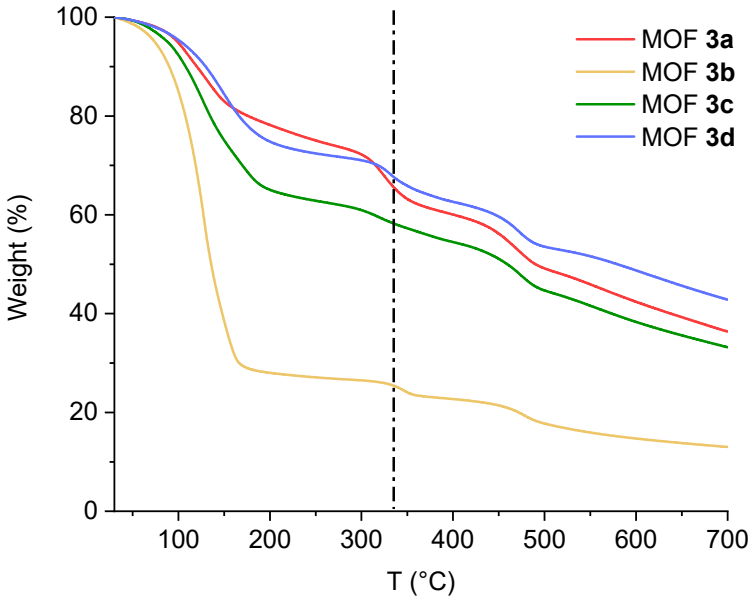

Figure S12. TGA profiles of as synthesized MOFs **3a**, **3b**, **3c** and **3d**.

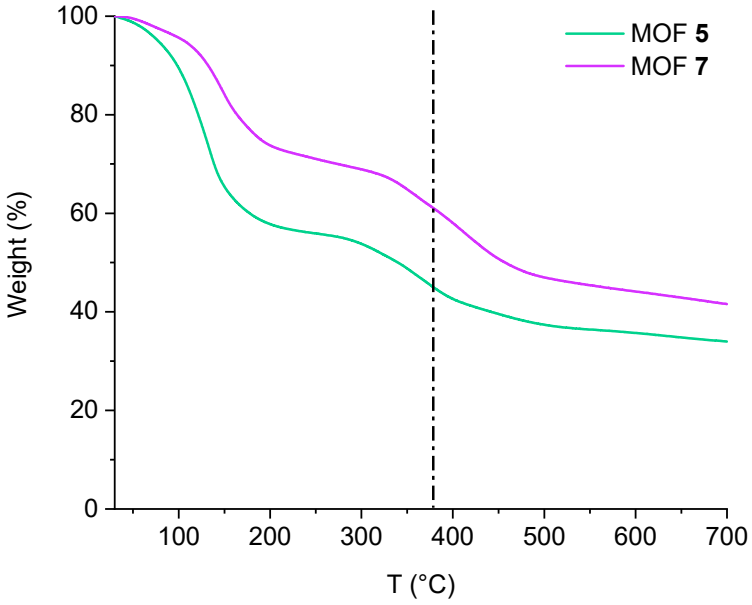

Figure S13. TGA profiles of as synthesized MOFs **5** and **7**.

PXRD analysis

For **Figures S14, S19** and **S21**: X-ray diffraction data obtained from Debye Scherrer measurements (in mother liquor) were treated using profile fits (Le Bail), taking unit cells as published.[5] Rietveld refinements were not successful due to numerous issues with the sample. As grinding was impossible due to the low mechanical stability the crystallite, sizes were very different, leading to both peak shape and certainly intensity issues when measuring with a 1D detector. A varying amount of guest molecules is likely another cause for intensity discrepancies with respect to the published structures.

Profile fits were done in Topas5 using the Le Bail method. Along with unit cell parameters, the zero shift, 6 profile parameters of a Pearson VII function and between 6-10 background terms were refined. MOF **4** "as synthesized" data were refined with the published MOF **4** tetragonal *P*4/*nmm* unit cell yielding slightly larger unit cell axes at present with *a* = *16*.7326(7) and *c* = 30.9532(8). MOF **6** "as synthesized" diffraction data were modelled using the published MOF **6** monoclinic *C*2/*m* unit cell. Again, a slight increase of unit cell axes is observed with respect to the published structure: *a* = 22.3337(4), *b* = 16.9242(9), *c* = 16.5134(6), *β* = 103.666(3). The resulting Le Bail fits are shown in **Figures S19** and **S21**. Data for MOF **1** did not match well the model based on the MOF **1** published unit cell. These data were re-indexed using FOX and then refined as above with the Le Bail method (**Figure S14**). The resulting parameters deviate slightly from the published structure in *a* and *b*, but match well in *c*, which is the pillaring direction: *a* = 11.307(2), *b* = 15.922(3), *c* = 22.423(2).

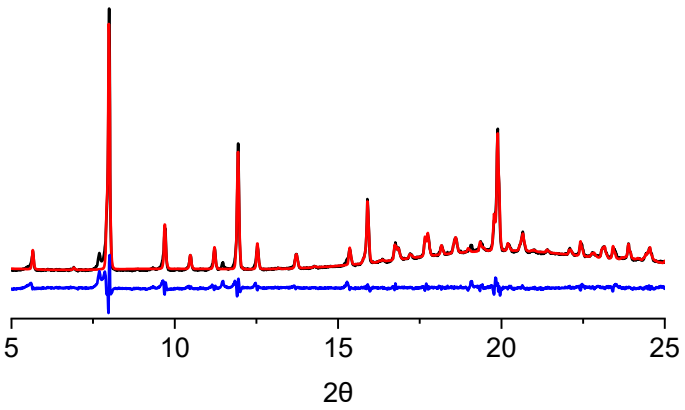

Figure S14. Comparison of PXRD patterns: **1** calculated (red), **1** observed (black) and the difference (blue).

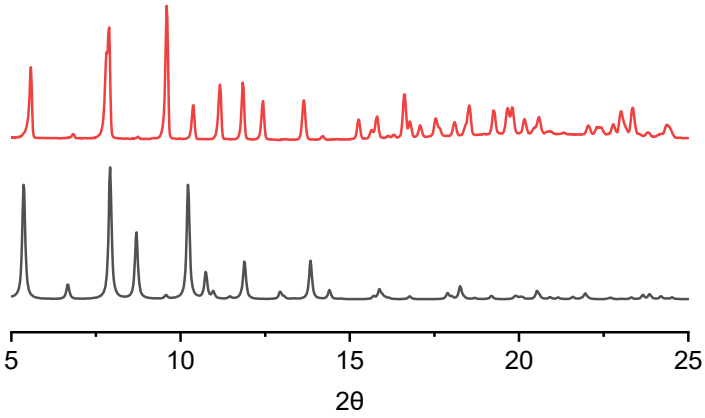

Figure S15. Comparison between **1** (black) as published and **3a** (red).

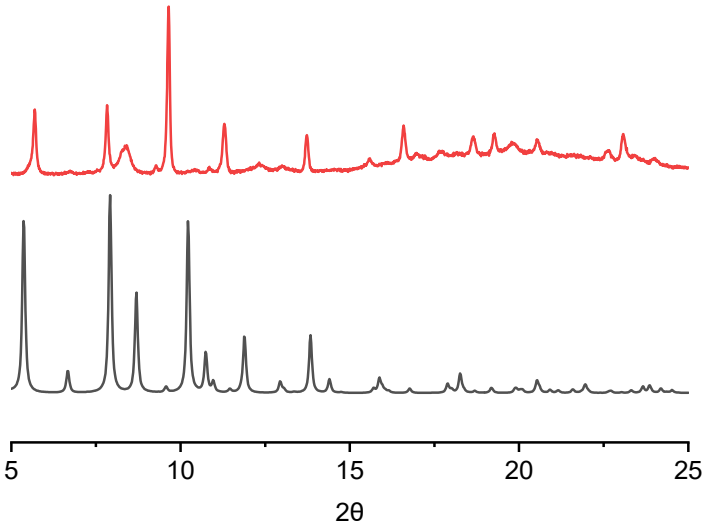

Figure S16. Comparison between **1** (black) as published and **3b** (red).

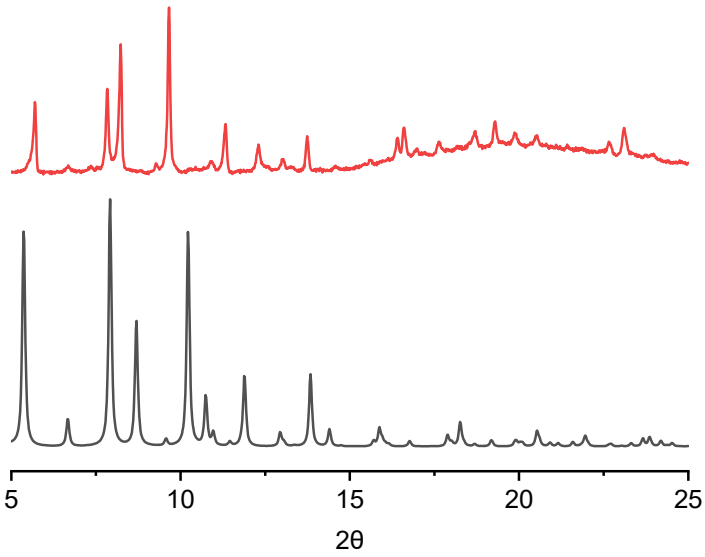

Figure S17. Comparison between **1** (black) as published and **3c** (red).

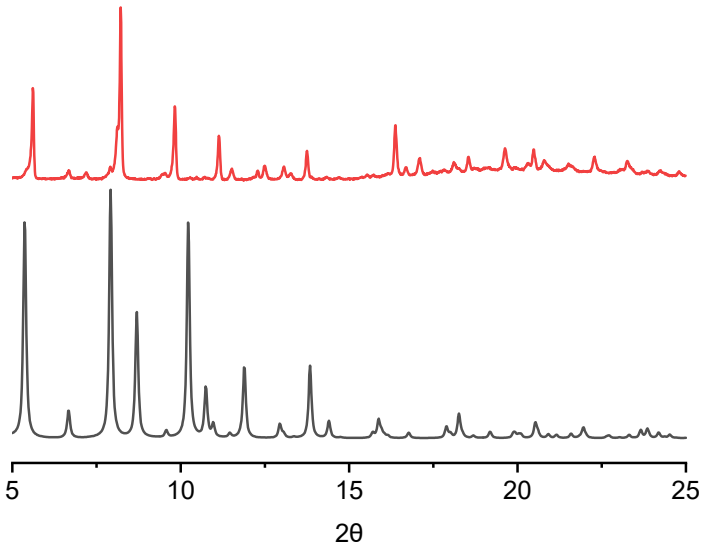

Figure S18. Comparison between **1** (black) as published and **3d** (red).

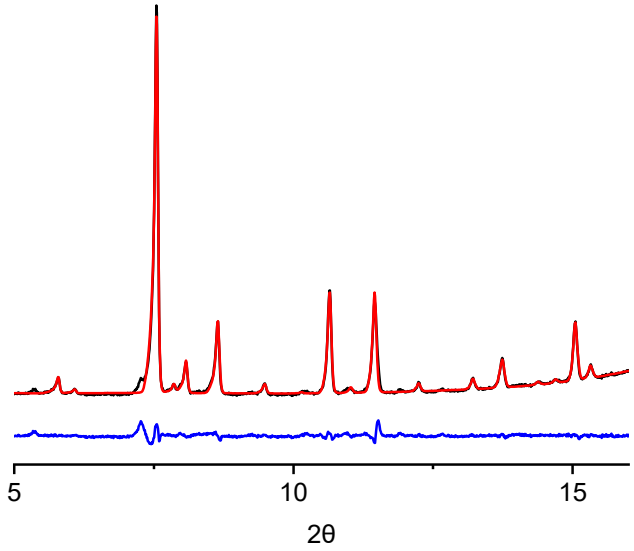

Figure S19. Comparison of PXRD patterns: **4** calculated (red), **4** observed (black) and the difference (blue).

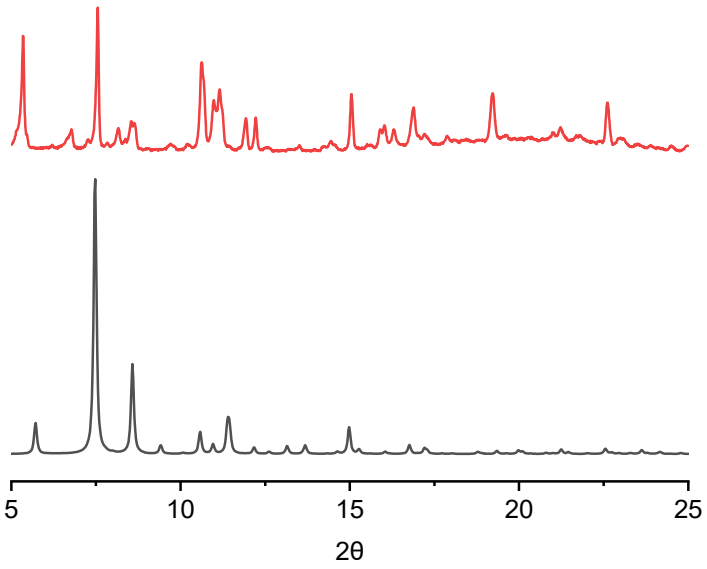

Figure S20. Comparison between **4** (black) as published and **5** (red).

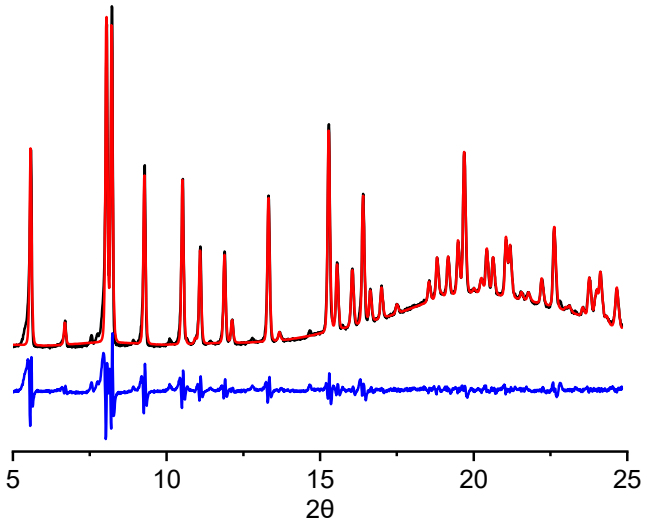

Figure S21. Comparison of PXRD patterns: **6** calculated (red), **6** observed (black) and the difference (blue).

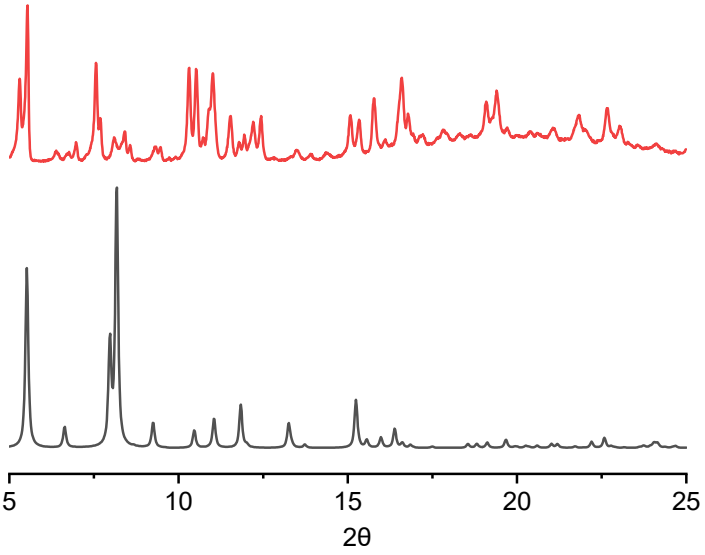

Figure S22. Comparison between **6** (black) as published and **7** (red).

Crystallographic data

Bragg-intensities of **3a**, **3d**, **5** and **7** were collected at different temperatures (See **Table S2**) using Cu *Kα* radiation. A Rigaku SuperNova dual system diffractometer with an Atlas CCD detector was used for compounds **3a** and **7**, and one equipped with an Atlas S2 CCD detector for compounds **3d** and **5**. The datasets were reduced and corrected for absorption, with the help of a set of faces enclosing the crystals as snugly as possible, with *CrysAlis*^{Pro}.[6]

The solutions and refinements of the structures were performed by the latest available version of *ShelXT* and *ShelXL*.[7,8] All non-hydrogen atoms were refined anisotropically using full-matrix least-squares based on $|F|^2$. The hydrogen atoms were placed at calculated positions by means of the "riding" model in which each H-atom was assigned a fixed isotropic displacement parameter with a value equal to 1.2 U_{eq} of its parent C-atom (1.5 U_{eq} for the methyl groups). This model failed, however, in **5** for all hydrogens and in **7** for those on the clathrochelate. This failure is due to the existence of orientational disorder compounded by the presence of reflection-symmetries (no reasonably complex molecule will crystallise in a space group such as *I*4/*mmm* without need).

Crystallographic and refinement data are summarized in **Table S2**. Crystallographic data have been deposited with the Cambridge Crystallographic Data Centre and correspond to the following codes: **3a** (1972501), **3d** (1972502), **5** (1972503) and **7** (1972505). These data can be obtained free of charge via www.ccdc.cam.ac.uk/data_request/cif, or by emailing data_request@ccdc.cam.ac.uk, or by contacting The Cambridge Crystallographic Data Centre, 12 Union Road, Cambridge CB2 1EZ, UK; fax: +44 1223 336033.

The structure of most MOFs are highly disordered in general. This disorder, due to orientational or dynamical disorder, voids and guest molecules, often generates reflection-symmetries further compounding the situation. Therefore, we are often facing broad and weak reflections, especially at high angles, resulting in a too low number of reflections and unsatisfactory confidence factors.

Additional electron density found in the difference Fourier map (due to highly disordered solvent molecules) was removed in all structures by help of the solvent-masking program in *OLEX2.*[9]

Table S2. X-ray crystallographic data for **3a**, **3d**, **5** and **7**.

Compound	**3a**	**3d**	**5**	**7**
Formula	$C_{50}H_{30}B_2Br_2FeN_8O_{14}Zn_2$	$C_{63}H_{46}B_2Br_2FeN_8O_{14}Zn_2$	$B_6C_{158}Fe_3N_{32}O_{34}Zn_6$	$C_{64}H_{32}B_2FeN_{12}O_{14}Zn_3$
$D_{calc.}$/ g cm^{-3}	0.556	0.654	0.489	0.403
μ/mm^{-1}	1.865	1.975	1.275	0.977
Formula Weight	1334.85	1507.11	3514.53	1466.59
Colour	clear intense orange	clear intense orange	clear dark purple	clear intense purple
Shape	prism	plate	plate	prism
Size/mm^3	0.52×0.20×0.08	0.55×0.18×0.07	0.49×0.34×0.05	0.55×0.18×0.13
T/K	210.00(10)	293(2)	200.00(10)	140.00(10)
Crystal System	orthorhombic	orthorhombic	tetragonal	orthorhombic
Space Group	*Pmmm*	*Pmmm*	*I*4/*mmm*	*Pmmm*
a/Å	11.6785(5)	10.9173(7)	16.71400(10)	16.2432(10)
b/Å	15.6070(4)	16.0826(7)	16.71400(10)	17.1019(17)
c/Å	21.8880(11)	21.8056(17)	85.4144(11)	21.7542(17)
α/°	90	90	90	90
β/°	90	90	90	90
γ/°	90	90	90	90
V/Å^3	3989.4(3)	3828.6(4)	23861.2(4)	6043.1(8)
Z	1	1	2	1
Z'	0.125	0.125	0.0625	0.125
Wavelength/Å	1.54184	1.54184	1.54184	1.54184
Radiation type	Cu $K\alpha$	Cu $K\alpha$	Cu $K\alpha$	Cu $K\alpha$
Θ_{min}/°	3.478	2.748	4.276	3.753
Θ_{max}/°	75.469	66.595	50.430	50.421
Measured Refl's.	25183	14886	51832	14293
Ind't Refl's	4416	3806	3632	3552
Refl's with I > 2(I)	3156	2840	3338	2744
R_{int}	0.0815	0.0498	0.0528	0.0731
Parameters	136	173	276	200
Restraints	260	323	704	421
Largest Peak/e Å^{-3}	1.957	3.223	2.220	4.430
Deepest Hole/e Å^{-3}	-1.521	-1.163	-1.101	-1.160
GooF	1.282	1.556	1.985	1.517
wR_2 (all data)	0.3362	0.3848	0.4001	0.3785
wR_2	0.3184	0.3671	0.3891	0.3593
R_1 (all data)	0.1201	0.1484	0.1136	0.1502
R_1	0.1063	0.1339	0.1096	0.1339
Total accessible volume/Å^3	2974.9	2332.5	17878.2	4794.2
CCDC code	1972501	1972502	1972503	1972505

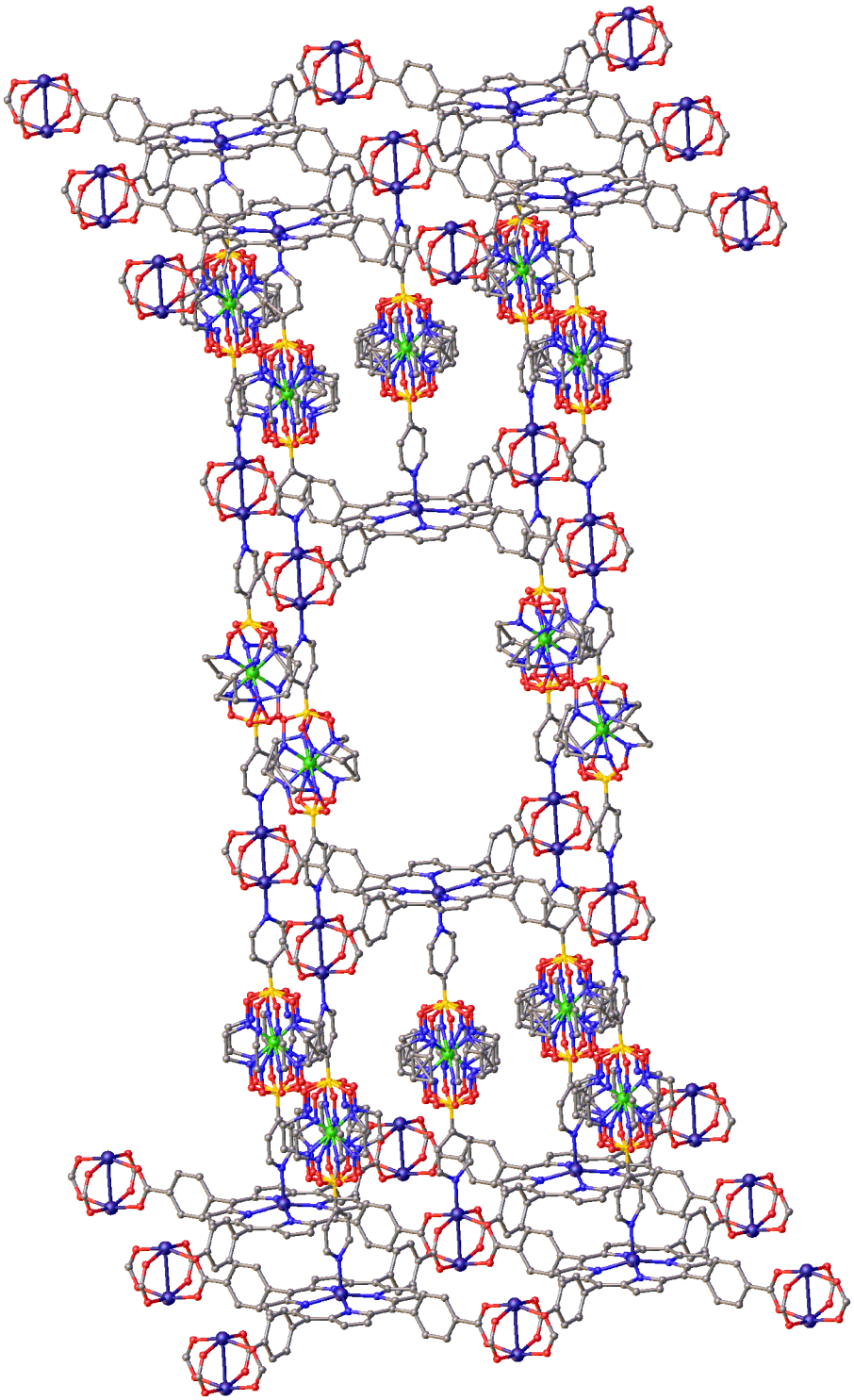

Figure S23. Part of the molecular structure of MOF **5** in the crystal. Color coding: C (gray), Fe (green), Zn (dark blue), O (red), B (yellow), N (blue). H atoms and solvent are omitted for clarity. Disorder around Fe is due to orientational or dynamical disorder.

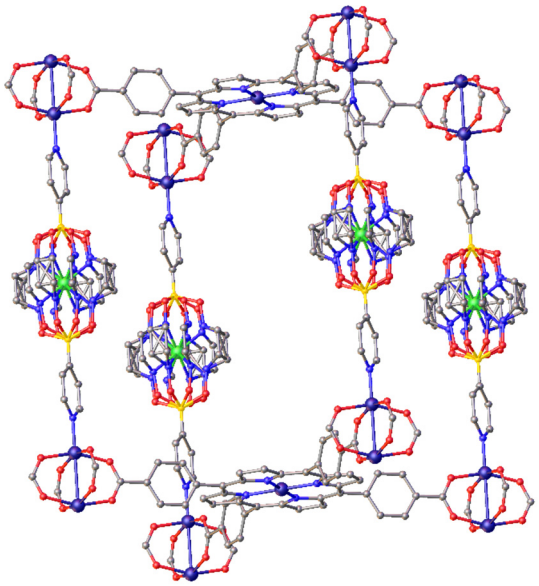

Figure S24. Part of the molecular structure of MOF **7** in the crystal. Color coding: C (gray), Fe (green), Zn (dark blue), O (red), B (yellow), N (blue). H atoms and solvent are omitted for clarity. Disorder around Fe is due to orientational or dynamical disorder.

References

1) Zelinskii, G. E.; Belov, A. S.; Vologzhanina, A. V.; Limarev, I. P.; Dorovatovskii, P. V.; Zubavichus, Y. V.; Lebed, E. G.; Voloshin, Y. Z.; Dedov, A. G. *Polyhedron* **2019**, 160, 108.
2) Bila, J. L.; Pijeat, J.; Ramorini, A.; Fadaei-Tirani, F.; Scopelliti, R.; Baudat, E.; Severin, K. *Dalton Trans.* **2019**, 48, 4582.
3) a) Lee, H. W.; Ji, S. K.; Lee, I. C.; Lee, J. H. *J. Org. Chem*. **1996**, 61, 2542; b) Pandey, R. K.; Upadhyay, R. K.; Shinde, S. S.; Kumar, P. *Synth. Commun*. **2004**, 34, 2323; c) Hofer, D.; Galanski, M.; Keppler, B. K. *Eur. J. Inorg. Chem*. **2017**, 2347.
4) Farha, O. K.; Malliakas, C. D.; Kanatzidis, M. G.; Hupp, J. T. *J. Am. Chem. Soc.* **2010**, 132, 3, 950.
5) Chung, H.; Barron, P. M.; Novotny, R. W.; Son, H.-T.; Hu, C.; Choe, W. *Cryst. Growth Des.* **2009**, 97, 3327.
6) CrysAlis^{Pro} Software System, Rigaku Oxford Diffraction, **2018**.
7) Sheldrick, G. M. *Acta Cryst.* **2015**, A71, 3.
8) Sheldrick, G. M. *Acta Cryst.* **2015**, C71, 3.
9) Dolomanov, O.V.; Bourhis, L. J.; Gildea, R. J.; Howard, J. A. K.; Puschmann, H. *J. Appl. Cryst.* **2009**, *42*, 339.